25th ABCM International Congress of Mechanical Engineering
October 20-25, 2019, Uberlândia, MG, Brazil

COB-2019-0662

STUDY OF THE POTENTIALITY TO MANUFACTURE FORMING TOOLS VIA WAAM (WIRE + ARC ADDITIVE MANUFACTURING)

Henrique Nardon Ferraresi
Fernando Matos Scotti
Universidade Federal de Uberlândia (UFU), Uberlândia, MG, Brasil.
henriquenardon@gmail.com, fernandomscotti@gmail.com

Américo Scotti
Universidade Federal de Uberlândia (UFU), Uberlândia, MG, Brasil/University West, Division of Welding Technology, Trollhättan, Suécia.
ascotti@ufu.br

Abstract. *Techniques for geometric customization and/or repair of tools such as punches and dies, without having to replace them, are of great interest in the mechanical forming industry. This work aims to show the potentiality to manufacture a metallic preform via WAAM (Wire +Arc Additive Manufacturing) over a cast iron substrate, in order to simulate a geometric customization of a cast iron bending tool set. For such, twelve layers of low carbon steel (AWS E70S-6 wire) were deposited over the nodular cast iron substrate through GMAW (Gas Metal Arc Welding) process. To achieve a functional interconnection between the cast iron and the steel, two intermediate layers (buttering) were deposited with an iron-nickel wire. The results show that it is possible to manufacture preforms with good regularity and geometric/dimensional tolerances. Regarding the microstructure, the most critical region is the PMZ (Partially Melted Zone), where there is ledeburite and carbides formation. Despite the high hardness, this microconstituents do not form a continuous lattice, hindering crack propagation. This was shown through Charpy impact tests where specimens notched at the PMZ region presented greater energy absorption compared to those notched at the base metal.*

Keywords: *Additive Manufacturing; WAAM; forming die; Nodular Cast Iron.*

1. INTRODUCTION

Agarwal et al. (2013) mentioned that a car chassis has around 300 stamped parts that went through over 700 stamping processes in different dies. For some applications, dies for automobile industry are made of cast iron, a relatively cheaper material, easier to cast and machine than a tool steel. The authors mention that an estimated economy of $300 for each car is achieved with the application of cast iron, instead of steel, in the making of the dies. However, around $30,000 are spent in repair over its life cycle. Facing this scenario, one can affirm that building preforms deposited layer by layer, instead of casting, could be economically gainful. This citation demonstrates the potential for the development of new technologies, such as WAAM (Wire + Arc Additive Manufacturing), aiming to minimize manufacturing and repair costs for dies.

Recent publications (CHEN et al., 2014, WILLIAMS, 2016 and DING et al., 2015) indicate the potential of applying WAAM with a variety of technologies (GMAW, GTAW, PAW) for geometric customization of punches and dies and building prismatic preforms over different materials such as, tool steel, cast iron and aluminum. Nevertheless, these works concentrate on the techniques and mechanical properties of the deposited geometry, while the effects caused on the substrate are still barely explored. Thus, there is a need to deepen the investigation on mechanical properties and microstructure of the base metal and substrate in WAAM.

This work has the objective of showing the potentiality of manufacturing carbon steel preforms over a cast iron substrate applying WAAM, in order to simulate the geometric customization of a nodular cast iron forming tool set. Specifically, this work aims at assessing the metallurgical behavior of the interconnection between the cast iron and the steel, when carried out by WAAM (potentially the critical point of the manufacture).

2. METODOLOGY

A die with a ‘U’ shaped cavity and the corresponding bending punch were designed, as shown in Fig. 1, as a case study. The building of the preforms used to manufacture the punch and die was made over a nodular cast iron (ASTM 247 standard) plate, with a predominantly pearlitic matrix, containing ferrite around the graphite nodules, as shown in the microstructure in Fig. 2, the substrate dimensions were 25 x 80 x 300 mm.

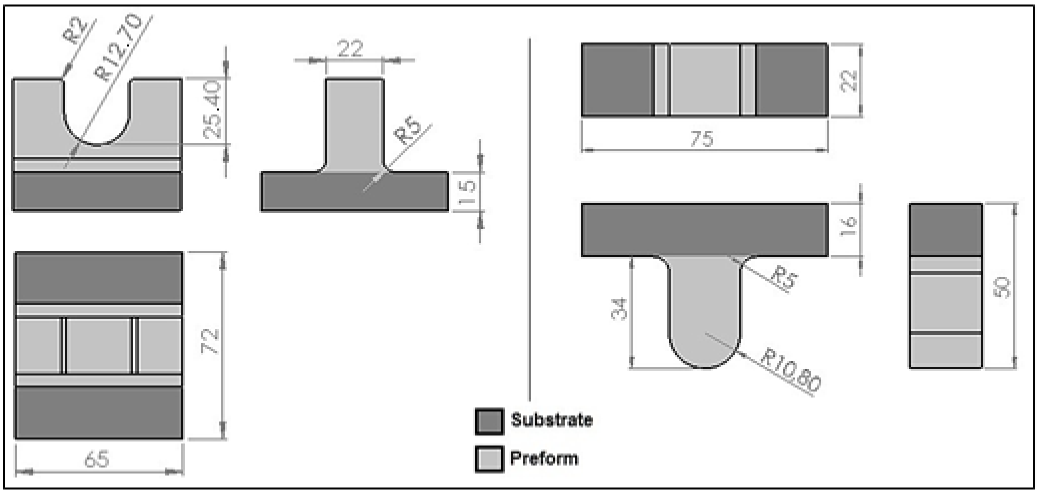

Figure 1. Die (left) and Punch (right) builds via WAAM (units in millimeters)

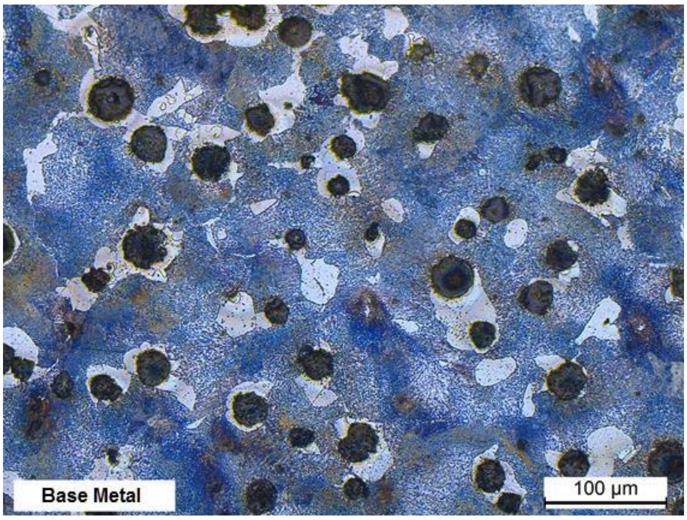

Figure 2. Typical microstructure of the base metal, composed by nodular graphite on a predominantly pearlitic matrix containing ferrite (chemical attack: Nital 3%)

Teixeira and Pope (1992) mentioned that welding or cladding with multiple layers results in a behavior similar to a heat treatment in the HAZ of the first previous (phenomenon known as tempering pass), when the following layer is deposited over the previous one, meaning, the heat generated in the application of the second layer can reduce hardness in the coarse grain region of the first layer HAZ in the base metal, reducing costs related to preheating and/or post-heating.

Thereby, in order to achieve an interconnection that does not deteriorate the properties of both substrate and deposited layers, two buttering layers were deposited with Nickel-Iron wire UTP A 8051 Ti (AWS A5.15). The choice of a niquel-based material (ductile) for the battering had the objective of accommodating by deformation the thermal stresses generated during the steel deposition, preventing cracks in the sensitive parts (heated affected zone, HAZ, and the partially melted zone, PMZ) of the substrate. The welding conditions for the buttering layers deposition are presented in Tab. 1. Fig. 3 shows the bead deposition sequence. The side overlap is 30% between beads.

Table 1. GMA welding and torch weaving parameters for buttering layer

Reference Voltage	19 V	Weaving Amplitude	6 mm
Electrode-Wire Feed Speed	4 m/min	Weaving Frequency	1 Hz
Welding Speed	25 cm/min	Protection Gas	Ar + 4%CO2
Contact-tip to work distance (CTWD)	14 mm	Work and Position Angle	90°

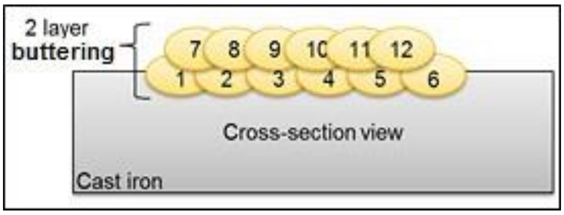

Figure 3. Illustration of two buttering layers numbered by deposition order, totaling 12 beads

Over the buttering layers, a prismatic geometry preform was built. For such, 12 layers were deposited with 5 beads each, totaling 60 beads with the low carbon wire AWS E70S-6, without weaving, with the welding parameters presented in Tab. 2. Figure 4 illustrates the weld bead deposition sequence, from the center to the edges, with 35% side overlap between beads.

Table 2. GMA welding parameters for the prismatic geometry deposition

Reference Voltage	19 V	Weaving Frequency and Amplitude	0 mm, 0 Hz
Electrode-Wire Feed Speed	3.5 m/min	Protection Gas	Ar + 25%CO2
Welding Speed	40 cm/min	Work and Position Angle	0°
Contact-tip to work distance (CTWD)	15 mm	Interpass Temperature	80 – 100°C

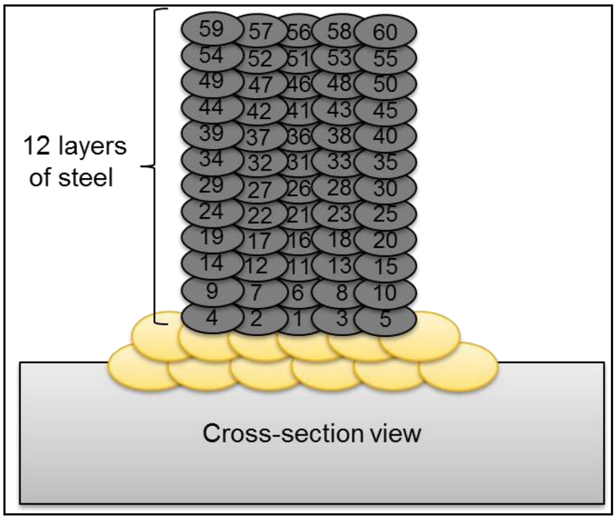

Figure 4. Illustration of the 12 steel layers numbered by deposition order, totaling 60 beads

Two pieces were cut from the built preform in order to manufacture the die and punch as designed and shown in Fig. 1. Moreover, three samples were cut for toughness evaluation through Charpy-V tests and one sample for microstructure and microhardness analysis.

3. RESULTS AND DISCUSSIONS

After the deposition of the two nickel-iron buttering layers and twelve steel layers, the resulting preform has few superficial imperfections, with good surface finish and average geometric-dimensional regularity as shown in Fig. 5.

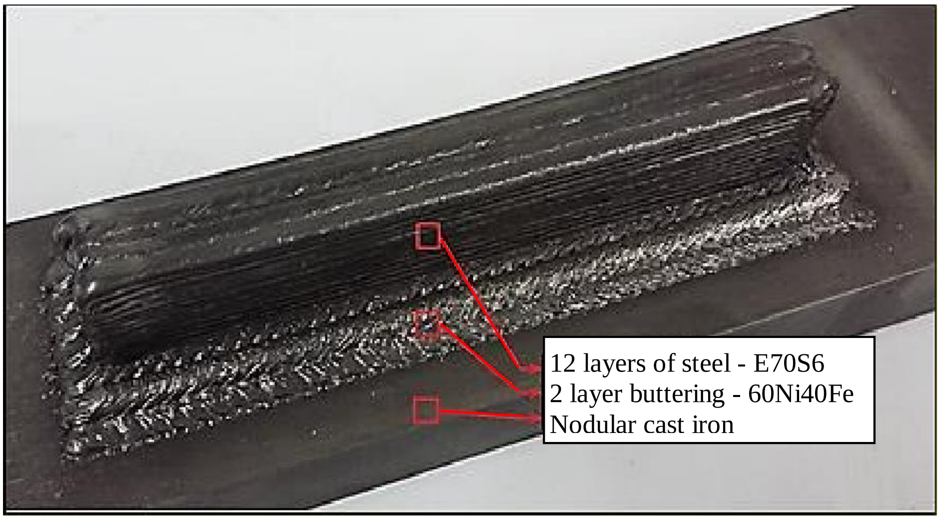

Figure 5. Perspective image of the steel wall built over a nodular cast iron with two intermediate buttering layers of iron-nickel alloy

3.1 Microstructure

A sample was cut from the built preform for microstructure analysis. The sample was ground by sand paper from 80 to 1200 mesh, polished with 1 and 0.5 μm Alumina, and chemically attacked with Nital 5%. Figure 6 shows the macrograph of the sample profile where it is possible to see the two layers of nickel formed over the cast iron substrate and the twelve layers of steel over the buttering layer.

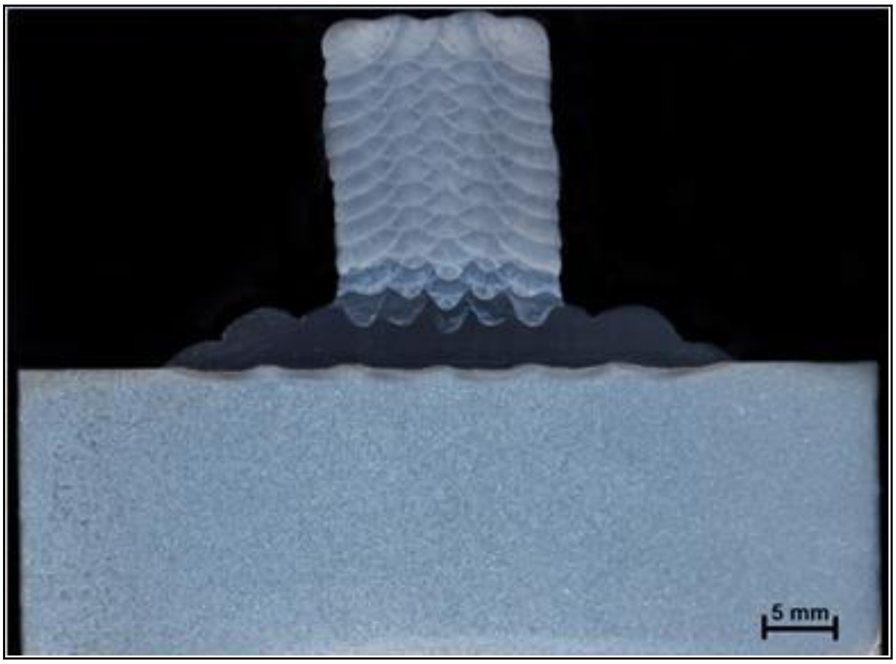

Figure 6. Macrograph of the prismatic preform profile

Figure 7 shows the micrograph of the interface between the heat affected substrate and the buttering layer. In this case, four regions can be distinguished: Fusion Zone (ZF); Partially Melted Zone (PMZ); High Temperature Heat-Affected Zone (HAZ); and Low Temperature Heat-Affected Zone (HAZ).

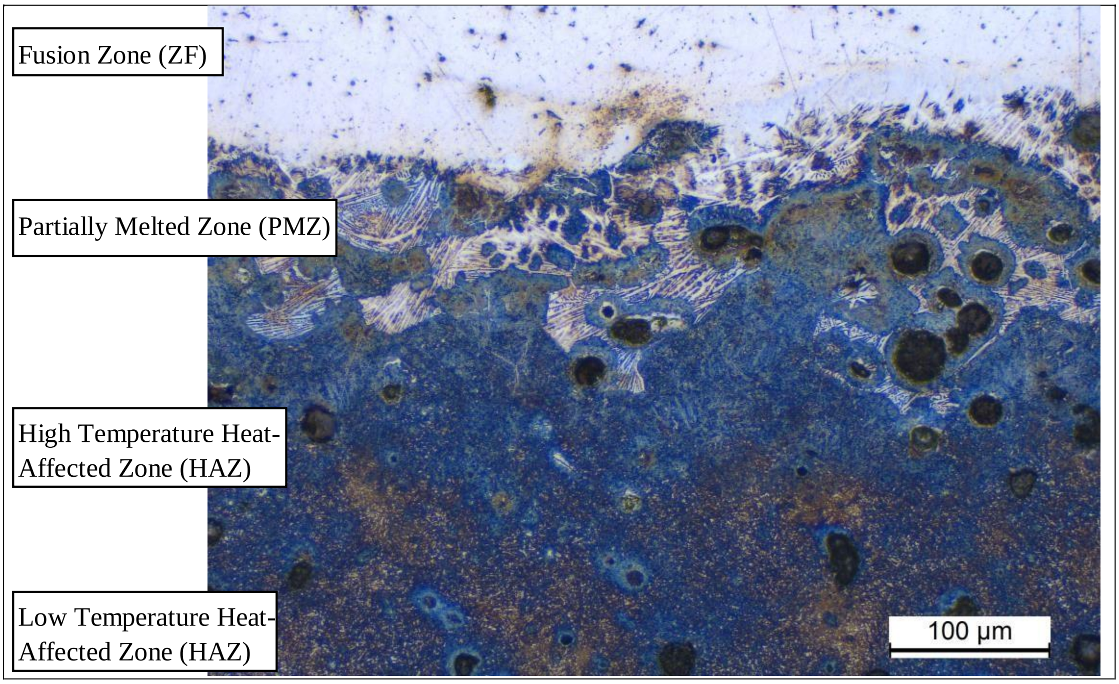

Figure 7. Typical microstructure of the interface between the first Nickel layer and the cast iron substrate

The dark dots noticeable in the FZ are graphite. According to ANSI/AWS D11.2-89, this phenomenon when welding cast iron is related to the presence of carbon in nickel, which does not form carbides and has low solid-state solubility. When the weld metal solidifies, the carbon is rejected from the solid solution, precipitating in the form of graphite. The PMZ region has around 200 µm and is composed of tempered martensite, carbides and ledeburite (pearlite globules over a cementite background), preferably around the graphite nodules. At the High Temperature HAZ, there is tempered martensite and, in the Low Temperature HAZ, there is diffusion of carbon to ferrite and small changes in the pearlite structure.

Regarding microstructure, the most critical region is the PMZ, where ledeburite and carbides are formed. Despite the high hardness, as will be seen later, these microconstituents do not form a continuous lattice, hindering a possible crack propagation. This fact is different from what would be observed in vermicular cast iron, for example, where the average distance between graphite worms is way less than the average distance between the carbon nodules, resulting in a continuous lattice of ledeburite and carbides, forming a preferential region for crack propagation.

3.2 Microhardness

A Vickers microhardness profile was made from the base metal region to the third steel layer, as shown in Fig.8. The load of 200 g was applied for 15 seconds. Position 0.0 mm is sitting on the fusion line. The regions are indicated by letters in the figure and correspond to: A - Base metal unaffected by heat (from -3.0 to -1.75 mm); B - Low Temperature HAZ (from -1.75 to -0.5 mm); C - High Temperature HAZ (from -0.5 to 0.25 mm); D - PMZ (from -0.25 to 0.0 mm); E - Nickel layers (from 0.0 to 4.5 mm); F - First steel layer (from 4.5 to 7.0 mm); G - Second steel layer (from 7.0 to 10.0 mm; H – Adjacent steel layers (from 10.0 mm to 20.0 mm).

On the PMZ (region D), the carbides and ledeburite have microhardness between 700 and 800 Vickers, way higher than the base metal, which can cause failure during service. Immediately to the right of the fusion line (region E) there is a drastic change in microhardness, corresponding to the nickel layers with average values of 200 Vickers. This region function is to absorb the thermal stresses during deposition and in the presence of the carbon from the cast iron it does not form carbides, avoiding crack nucleation.

The variations in microhardness of the steel layers are still not widely understood, the fused zone of the first layer correspond to the heat affected zone of the subsequent layers and the side beads. Thus, this region presents a wide variation in microstructure due to the multiple thermal cycles. Regarding the microstructure the most critical region is also the PMZ, where the ledeburite and carbides have elevated hardness. Leading to the conclusion that the most daunting challenge in WAAM of cast iron is neither actually the geometry nor the preform microstructure, but the interconnection region between the cast iron and other materials that in under the heat imposed by the arc transforms into brittle microconstituents with elevated hardness.

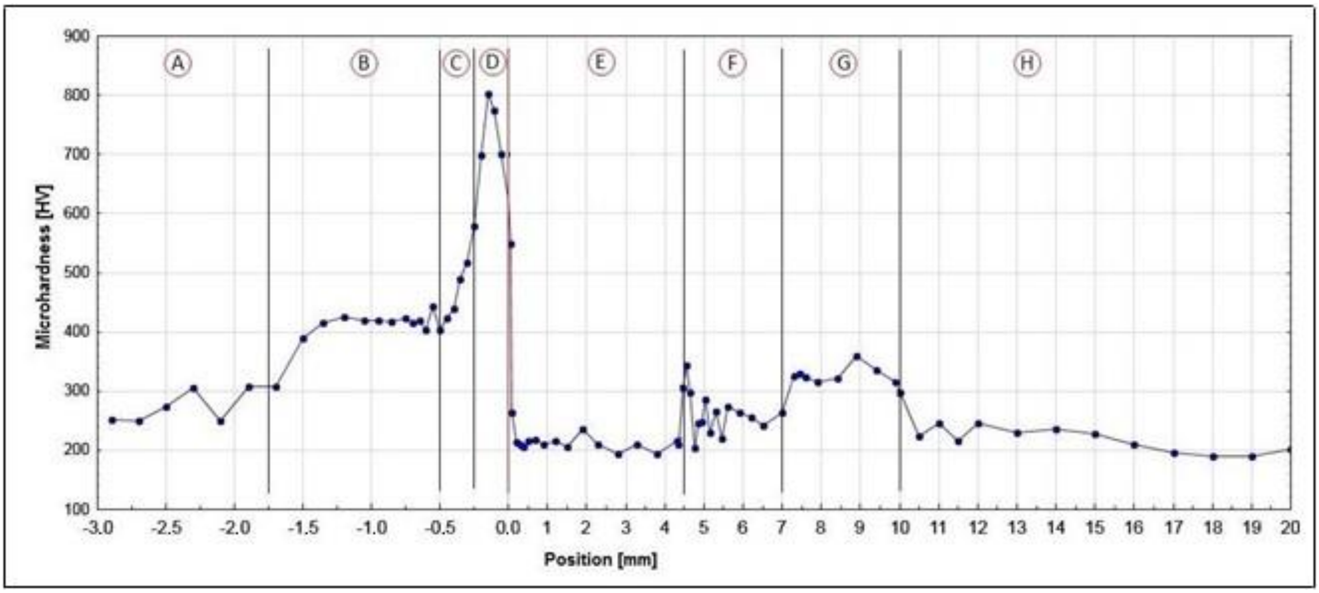

Figure 8. Microhardness profile of a transverse section central line in the prismatic preform height direction. The position 0.0 mm is the fusion line

3.4 Toughness

The Charpy-V impact tests and the respective specimens' dimensions were made accordingly to NBR ISO 148-1 (10/2013), denominated "Metallic Materials – Impact tests through pendulum Charpy - Part 1: Test method". The specimens have 55 mm in length and a square profile with 10 mm sides, with a V notch centered, made with a milling machine. One specimen was cut from the substrate (specimen 1) and three others (specimens 2, 3 e 4), sampling the same location, were cut from the preform and attempted notched on the partially melted zone (PMZ) between the substrate and the first layer of buttering, as shown in Fig. 9.

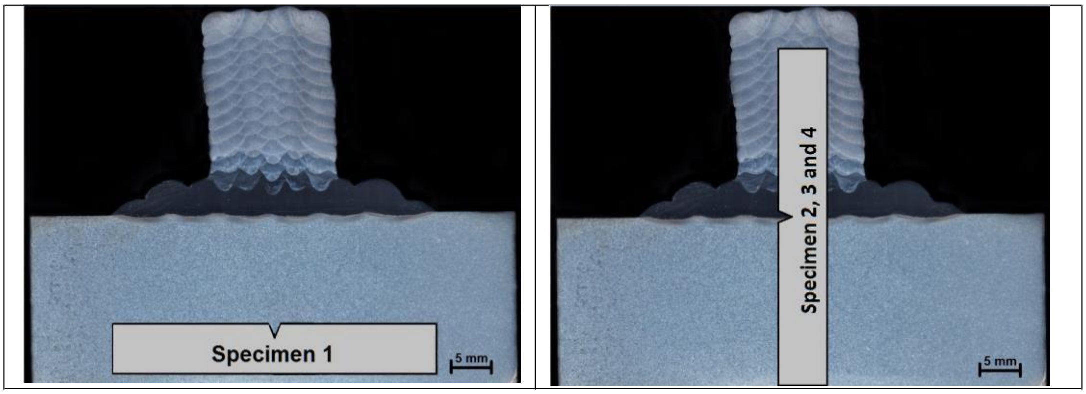

Figure 9. Cutting position of the specimen for Charpy-V tests

Table 3 and Fig. 10 show the toughness test results. For the specimen notched at the base metal the total absorbed energy is in accordance with the literature (Oliveira et al., 2017), the crystalline aspect of the fracture surface, show in Fig. 11, suggests brittle fracture, with 100% of cleavage. Specimens 2, 3 and 4 absorbed more energy, with fractures presenting crystalline and fibrous aspect, as shown in Figs. 12, 13 and 14. The specimens 2 and 3 had 75% and 50% of cleavage, respectively. On specimen 4 it was not possible to calculate the ductile-brittle fracture percentage with proper assurance.

The tendency to increase absorbed energy in the specimens notched at the PMZ, along with the fibrous aspect of the fracture surface, suggest the presence of a tougher microconstituents, such as tempered martensite. The deviation between specimens 2 and 4 are due to the difficulty of maintaining the notch in the desired position, since there is a very hard region followed by a very soft region.

Table 3. Absorbed energy in Charpy-V test as a function of the notch position

Specimen number	Location notch	Absorbed Energy (J)	Mean (J)	Standard deviation (J)
1	Base Metal	5.88	5.88	-
2	PMZ	6.86	8.49	2.04
3		10.78		
4		7.84		

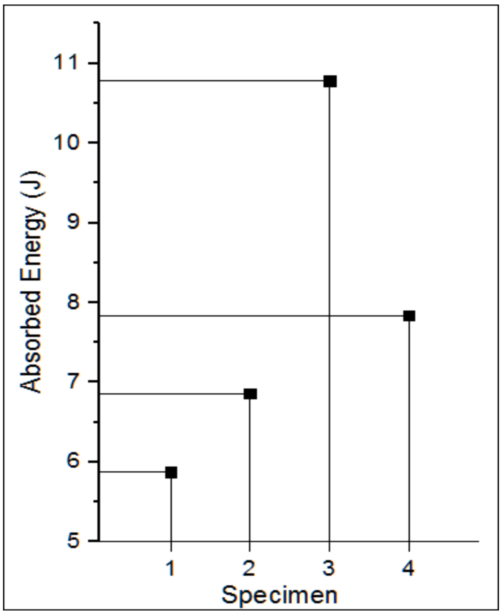

Figure 10. Resulted Charpy

Figure 11. Fractography of Specimen 1

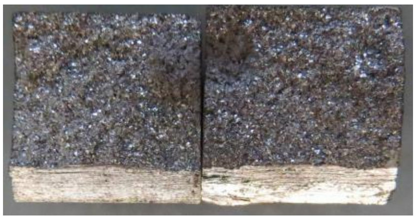

Figure 12. Fractography of Specimen 2

Figure 13. Fractography of Specimen 3

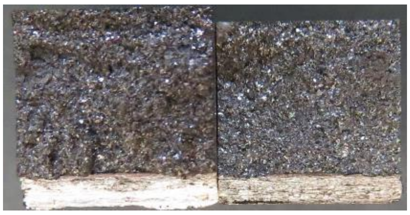

Figure 14. Fractography of Specimen 4

Charpy testes shown that despite the microstructure and the severity of microhardness at the PMZ, the region absorbed more energy than the base material, proving that despite the microconstituents with elevated hardness, due to the fact that they do not constitute a continuous lattice and the presence of streaky tempered martensite, hindering crack propagation.

4. Functionality tests of the bending tool set manufactured via WAAM

Two bulk pieces were cut from the built prismatic preform. From these, the ‘U’ shaped die cavity and the punch shown in Fig. 15 were machined. Bending tests were carried out as to prove the functionality of the built fixtures. Six ferritic stainless steel (UNS 43932) sheets were used. Table 4 shows the chemical composition and dimensions of the sheets.

Table 4. Nominal chemical composition of the metal sheets (*) used in the die functionality tests

Cr	C	N	Ti	S	Nb
17.050	0.011	0.013	0.2	0.002	0.190

** From ArcelorMittal*

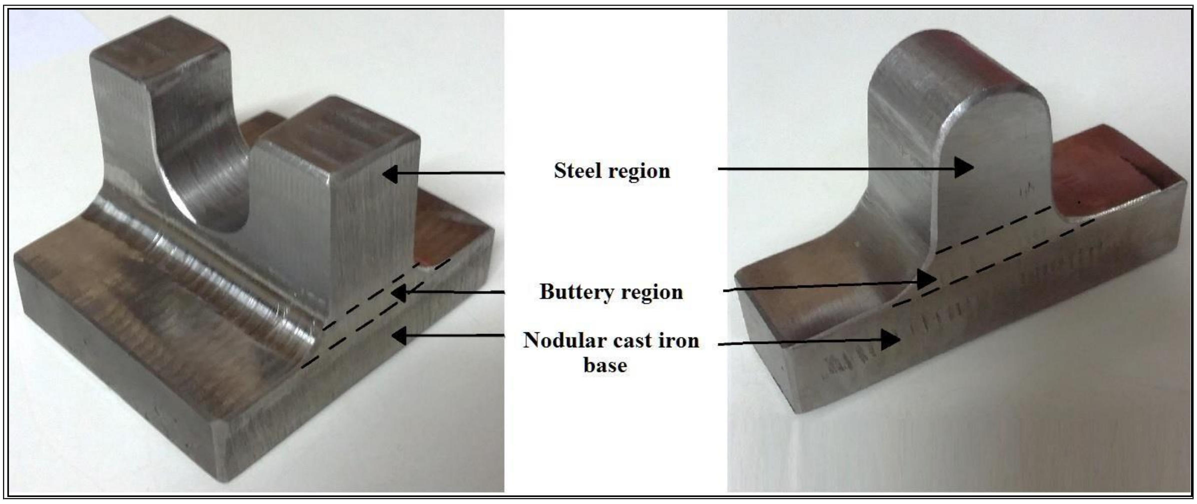

Figure 15. Die (Left) and Punch (Right) manufactured based on WAAM built preforms with indicated regions

The die and punch were aligned and fixed into a manual hydraulic press with 11 ton of capacity, with 100 kg resolution. The load is given by the manual lever and is shown by an analogic manometer. The six tests were held in ambient temperature. The necessary load to bend the stainless steel sheets was around 150 Kg. In order to test the tools at the end of each bending operation, load was applied until reaching 800 Kg. Figure 16 shows a sequence of three images representing the steps of a complete bending test. After the tests, there was no distortion of the components, indicating a strong potential of the application of WAAM with nodular cast iron.

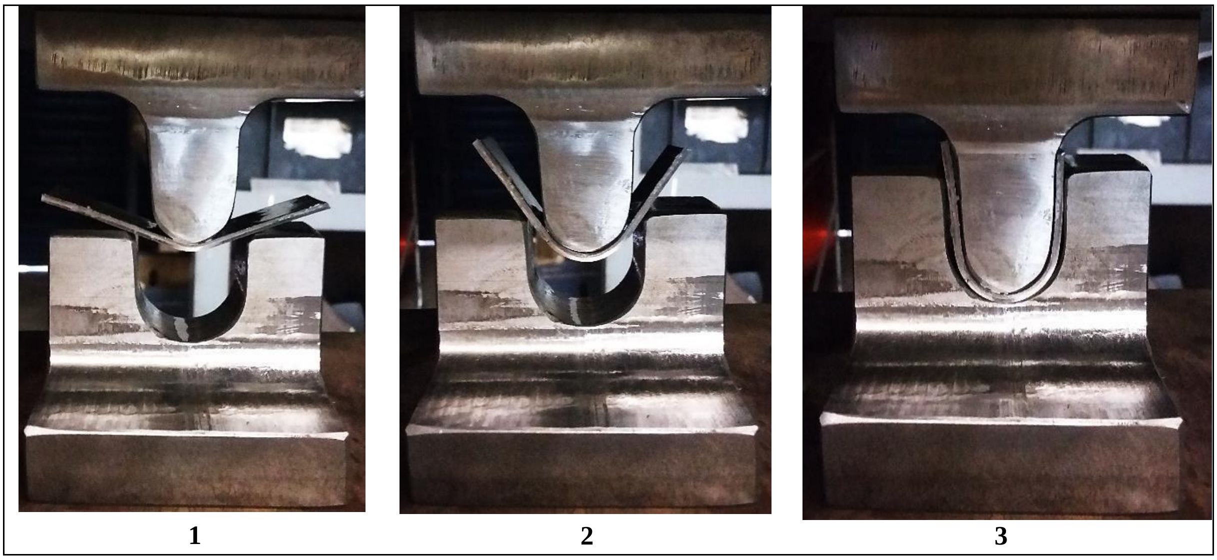

Figure 16. Bending test sequence

5. CONCLUSIONS

The main objective of showing the potential use of WAAM for geometric customization of punches and dies with a nodular cast iron substrate was achieved. A functional bending tool set prototype, consisting of a die with an ‘U’ shaped cavity and a punch, was built and assessed. Allowing the simulation of sheet metal forming operations, in which the prototype did not present any failure or distortion of the components.

Moreover, the results were complemented by the microstructure and toughness assessment. It was shown that despite the still elevated hardness at the PMZ (Partially Melted Zone), considering the effect of tempering pass of the buttering layer, the microstructural arrange of the ledeburite and carbides along with the streaky tempered martensite, resulted in higher toughness which tended to absorb more energy on the impact test when compared to the base metal.

6. ACKNOWLEDGEMENTS

This research was funded by CAPES, grant number 001, and the National Council for Scientific and Technological Development – CNPq, grant numbers 302863/2016-8. The authors would like to thank these Brazilian agencies for awarding research and study grant and the Federal University of Uberlândia, through the Mechanical Engineering Graduate Program, for financing the participation in COBEM 2019.

7. REFERENCES

AGARWAL K. et al. DC pulsed plasma deposition of nanocomposite coatings for improved tribology of gray cast iron stamping die. Journal of Materials Processing Technology. v.213, pp. 864-876. 2013. 10.1016/j.jmatprotec.2013.01.002.

CHEN, C. et al. A Review on Remanufacture of Dies and Molds. **Journal of Cleaner Production**. v.64, p.13-23. 2014. https://doi.org/10.1016/j.jclepro.2013.09.014;

WILLIAMS, S. **Use of WAAM for Manufacture of Reconfigureble Tooling with Conformal Features**. England: Welding Engineering and LASER Processing Centre - Cranfield University. Out. 2015. 3p. Disponível em: <https://waammat.com/documents/waam-for-tooling-applications>. Access in: 01 de jul. de 2016;

DING, D. et al. Wire-feed Additive Manufacturing of Metal Components: Technologies, Developments and Future Interests. **The International Journal of Advanced Manufacturing Technology**. London: v.85, n.1-4, p.465-481. 2015;

TEIXEIRA, J. C. G.; POPE, A. M. Técnica de Deposição em Dupla-Camada para Reparo e Modificações e Tratamento Térmico Pós-Soldagem de Aço 1Cr-0,5Mo. **Soldagem e Materiais**, v.4, n.2, p.23-27. 1992;

AMERICAN SOCIETY FOR TESTING AND MATERIALS. **ASTM A247-17**: Standard Test Method for Evaluating the Microstructure of Graphite in Iron Castings. USA, 2017. 13p;

AMERICAN WELDING SOCIETY. **D11.2-89**: Guide For Welding Iron Castings. USA, 1989. 208p;

OLIVEIRA, A. R de F.; BASTOS, P. M.; SILVA, F. R.; SILVA, F. R. R. In: Simpósio do Programa de Pós-graduação em Engenharia Mecânica, 27, 11 a 13 de Setembro, Uberlândia. **Análise de Impacto Charpy em Corpos de Prova de Ferros Fundidos.** Universidade Federal de Uberlândia, 2017.

5. RESPONSIBILITY NOTICE

The authors Henrique Nardon Ferraresi, Américo Scotti and Fernando Scotti are the only responsible for the printed material included in this paper.